



Origin and value of a limit size during shear aggregation revisited

Frédéric Gruy

► **To cite this version:**

Frédéric Gruy. Origin and value of a limit size during shear aggregation revisited. 2006. <hal-00906461>

HAL Id: hal-00906461

<https://hal.archives-ouvertes.fr/hal-00906461>

Submitted on 19 Nov 2013

HAL is a multi-disciplinary open access archive for the deposit and dissemination of scientific research documents, whether they are published or not. The documents may come from teaching and research institutions in France or abroad, or from public or private research centers.

L'archive ouverte pluridisciplinaire **HAL**, est destinée au dépôt et à la diffusion de documents scientifiques de niveau recherche, publiés ou non, émanant des établissements d'enseignement et de recherche français ou étrangers, des laboratoires publics ou privés.

Origin and value of a limit size during shear aggregation revisited

Frédéric GRUY

Ecole des Mines de Saint-Etienne, 158 Cours Fauriel,

42023 SAINT ETIENNE Cedex 2, FRANCE

running title :

correspondence : Prof. F. Gruy

Ecole des Mines de Saint-Etienne, 158 Cours Fauriel,

42023 SAINT ETIENNE Cedex 2, FRANCE

Abstract

During the aggregation of fine particles in a shear flow a limit size value a_L for aggregates is reached. Most researchers have related a_L to the shear rate $\dot{\gamma}$ by means of a power law. We examine in this paper the different ways in order to model the phenomena leading to a limit size. The main results in the field of drop-drop and bubble-particle systems are briefly reviewed to help us to propose a coherent description of phenomena occurring in particle-particle systems. Kernels for coalescence, aggregation, breakage and erosion are recalled. An improvement of the aggregation kernel in the case of the collision between aggregates is proposed. We show that an analysis of the whole process in term of aggregation-fragmentation competition will be preferred to a collision which would be less efficient between large aggregates. In this framework we present a modelling relating aggregation kernel and fragmentation kernel to a limit size value. As a consequence, the main result is the exponent value of the $a_L - \dot{\gamma}$ power law.

KEY WORDS : shear aggregation, limit size, aggregation kernel, fragmentation kernel

1. Introduction

Aggregation occurs in many biological, chemical and physical processes. It often concerns suspension of small particles in a liquid. Dynamics of aggregation mainly depends on the hydrodynamic conditions and on the particle size. In many practical situations, it is necessary to put the solid-liquid suspension on motion in order to homogenise or to convey it. In this case, whatever the nature (laminar or turbulent) of the flow, the role of the local shear flow in collisions becomes predominant. The collisions lead to the formation of aggregates. It has been observed that a limit size is reached for aggregates. The higher the shear rate $\dot{\gamma}$, the smaller the limit size a_L . The causes of the existence of a limit size value are not so clear. This can be due to two reasons : breakage or collision efficiency becoming zero beyond a critical size. Even if only partial results are available concerning the relation between the limit size and the shear rate, all researchers agree with a relation expressed as a power law. However, they propose different criteria (time, force or energy) to get it. Another problem lies in the link between the exponent and other characteristic parameters of aggregation-fragmentation. This paper attempts to bring answers to these three questions.

It is organised as follows : after a brief presentation of the theoretical background connected with aggregation and fragmentation of solid particles, previous results in the field of other dispersed media (drop-drop system and particle-bubble system) will be reminded. Then, we will present a survey of experimental data and results of modelling for $a_L - \dot{\gamma}$ relation for solid particle system ; at last, we will propose a general expression for $a_L - \dot{\gamma}$ relation, which will be discussed.

2. Theoretical background concerning solid particle suspensions

2.1. Aggregation

Aggregation is the consequence of a collision between particles. The mechanism which brings particles into close proximity results from the hydrodynamics of the suspension. An aggregate is characterised by its number i of primary particles (supposed identical). Aggregation between i -mer and j -mer may be represented by the quasi chemical equation :



The corresponding reaction rate can be written as :

$$\frac{dN_{i+j}}{dt} = K_{i,j}^{agg} N_i N_j \quad (1)$$

where $K_{i,j}^{agg}$ is the kinetic constant, also known as kernel. $K_{i,j}^{agg}$ contains two contributions : the particle-particle collision frequency $K_{0,i,j}^{agg}$ and the aggregation efficiency $\alpha_{i,j}^{agg}$:

$$K_{i,j}^{agg} = K_{0,i,j}^{agg} \alpha_{i,j}^{agg} \quad (2)$$

The particle-particle collision frequency function $K_{0,i,j}^{agg}$ is depending on the origin of the encounters between particles : Brownian motion, differential settling velocity, shear flow. The collision efficiency, $\alpha_{i,j}^{agg}$, depends on the different interactions between particles : physical forces and hydrodynamic resistance.

The morphology of the aggregates depends on the physicochemical and hydrodynamic conditions of their formation, as well as on their intrinsic mechanical properties. However the aggregation dynamics also depend on the morphology of the colliding particles. Experiments have shown that aggregates have a fractal structure (see for instance [1,2]).

An aggregate containing i primary particles of radius a_1 is characterised by : its fractal dimension D_f , its outer radius a_i and its hydrodynamic radius a_{Hi} ; as the structure of the aggregates is non-uniform, their volume density $\phi_a(r)$ depends on the distance r from the centre of mass of the aggregate ; the average volume density is written $\bar{\phi}_a$. These different characteristics are linked by the following relations [3] :

$$a_i = a_1 \left(\frac{i}{S} \right)^{\frac{1}{D_f}} \quad (3)$$

$$\phi_a(r) = \frac{S}{3} D_f \left(\frac{r}{a_1} \right)^{D_f-3} \quad (4)$$

$$\bar{\phi}_a = S \left(\frac{a_i}{a_1} \right)^{D_f-3} \quad (5)$$

where S is a structure factor, which is a function of D_f [3].

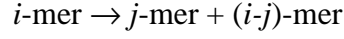
2.2. Fragmentation of aggregates

In the aggregation processes, aggregates usually reach a maximum size. This is due to two reasons : a breakage or a collision efficiency becoming zero beyond a critical size.

2.2.1. Breakage

The occurrence of breakage depends on the balance between the desaggregation effects due to the action of the fluid, and the overall cohesion of the aggregate due to the interactions between primary particles. The hydrodynamic effects are of different natures depending if the aggregate is larger or smaller than the Kolmogorov microscale.

Fragmentation of i -mer into two fragments $(i-j)$ -mer and j -mer may be represented by the quasi chemical equation :



The corresponding reaction rate can be written as :

$$\frac{dN_i}{dt} = K_i^{frag} N_i \quad (6)$$

where K_i^{frag} is the kinetic constant, or kernel, for fragmentation. K_i^{frag} contains two contributions : the eddy-particle collision frequency $K_{0,i}^{frag}$ and the fragmentation efficiency

α_i^{frag} :

$$K_i^{frag} = K_{0,i}^{frag} \alpha_i^{frag} \quad (7)$$

A topic still under discussion is relative to the size of the fragments produced by breakage.

Two cases are currently envisaged :

- the erosion of single or small groups of primary particles from the aggregate surface [4] ;
- the production of equisized fragments [5,6].

In all cases, the breakage rate depends on the hydrodynamic conditions of the flow and on the characteristics of the aggregates : outer radius, fractal dimension, primary particle radius and cohesion force between two primary particles.

The competition between aggregation and fragmentation leads to a steady particle size distribution (PSD). The corresponding mean particle size a_L depends on shear rate, according to :

$$\frac{a_L}{a_1} \propto \dot{\gamma}^{-m} \quad (8)$$

with $0 < m < 1$

2.2.2. Zero collision efficiency

This approach was especially developed by Brakalov [7]. The collision efficiency between two spherical particles of the same size decreases with their particle size. The decrease is sharper when the particles are porous which is the case for the aggregates. Otherwise one aggregate, which results from two smaller aggregates, can be too loose to survive. Brakalov showed that it exists a limit value for the aggregate size. However, the assumption of an additional short range interaction force was necessary to interpret the experimental results.

2.3. Restructuring of aggregates

Restructuring occurs during aggregation. Restructuring, that is a dynamic process, leads to a densification of aggregate, i.e an increase of contact numbers in aggregate. Two mechanisms are possible : the rolling of primary particles into aggregates due to the motion of the fluid or the rupture into fragments followed by reaggregation. Restructuring is characterized by an increase of the fractal dimension with time. At long time, fractal dimension value reaches a plateau. Selomulya et al. [8,9] proposed an empirical law for the change of fractal dimension versus time. Their main result was that no restructuring (constant low fractal dimension) occurs at low shear, whereas very fast restructuring (constant high fractal dimension) occurs at high shear, while restructuring competes, in a complex way, with aggregation and fragmentation at intermediate shear. But intensity of restructuring depends on the primary particle size. As the aggregate limit size is measured at long term, this corresponds to the maximum fractal dimension. So the latter increases with shear rate, as observed by [9-12].

3. Previous results for other dispersed media

Before studying the behaviour of solid particle suspension under shear flow it is interesting to examine two related topics :

- the coalescence and breakage of emulsion drops in turbulent medium
- the collection of particles by large bubbles in flotation process

This preliminaries will be followed by the study of aggregation-fragmentation in solid particle suspension.

3.1. Drop-drop system

Drops (with diameter d) undergo coalescence and fragmentation in an emulsion submitted to turbulence. The emulsion is characterized by the interfacial tension σ , by the density and the dynamic viscosity of the continuous phase (ρ_c, μ_c) and of the dispersed phase (ρ_d, μ_d).

Turbulence is characterized by the turbulent dissipation rate ε and the Kolmogorov scale λ_K .

3.1.1. Coalescence

The coalescence Kernel can be written, following Ross' equation [13] similar to equation (2), by :

$$K^{coal} = K_0^{coal} \alpha^{coal} \quad (9)$$

$$\text{with } \alpha^{coal} = \exp\left(-\frac{t_{coal}}{t_{contact}}\right) \quad (10)$$

The term K_0^{coal} is coming from the classical work of Saffman and Turner [14] for $d < \lambda_K$ or Abrahamson [15] for $d > \lambda_K$. Coalescence efficiency α^{coal} contains two characteristic times : the contact time and the coalescence time. The contact time depending on hydrodynamics only is given by :

$$t_{contact} \propto 2d / \sqrt{u^2(2d)} \quad (11)$$

where $\overline{u^2(\lambda)}$ is the mean square velocity difference between two points separated by the distance λ .

The coalescence time is expressed depending on the drop deformability :

For a deformable drop :

$$t_{coal} \propto \frac{\mu_c \overline{F}}{\sigma^2} f(h_0, h_c) d^2 \quad (12)$$

where \overline{F} is the hydrodynamic force acting on the two colliding drops :

$$\overline{F} \propto \rho_d \overline{u^2(2d)} d^2 \quad (13)$$

$f(h_0, h_c)$ is an expression related to the drainage of the liquid film, of which thickness varies between the initial value h_0 and the critical or final value h_c .

For a rigid drop :

$$t_{coal} \propto \frac{\mu_c}{F} d^2 \quad (14)$$

Recently, Narsimhan [16] proposed a modelling of drops coalescence in a turbulent medium. Drops were considered as rigid particles. He wrote the kinetic constant of coalescence as in equation (9).

The K_0^{coal} was also coming from Saffman and Turner for $d < \lambda_K$. Narsimhan presented coalescence as a collision governed only by the fluid motion leading to the formation of a doublet ; then the doublet might separate with a kinetic constant k_{sep} thanks to turbulence, or associate with a kinetic constant k_{ass} due to both turbulence and interaction forces. The association was followed by a very fast coalescence. So the coalescence efficiency could be written by :

$$\alpha^{coal} = k_{ass} / k_{sep} \quad (15)$$

Because repulsive and attractive forces were considered, the two-drop system presented an energy barrier which had to be overcome by turbulence to conduct to coalescence. By using the theory of stochastic processes he showed that :

$$k_{sep} = 2.7\sqrt{u^2(d)}/d \quad (16)$$

Association was studied in a similar way as the trajectory analysis [17], where the drop-drop distance h obeyed an ordinary differential equation :

$$dh/dt = -8h/(3\pi\mu_c d^2)(\bar{F} + F' + F_{int}) \quad (17)$$

$$\text{with } \bar{F} = \rho_d \overline{u^2(h)} \pi d^2 / 4 \quad (18)$$

and $h = h_{(F_{int}=0)}$ at $t = 0$

\bar{F}, F', F_{int} were respectively the mean turbulent (attractive) force, the fluctuating turbulent force and the interaction forces. Narsimhan considered that coalescence was instantaneous when the two drops were so close that the attractive interaction force became stronger than the repulsive one ($F_{int} < 0$). He deduced from (17) the expression of the mean association time

k_{ass}^{-1} . So he showed that association or coalescence time became dramatically long when :

$$\bar{F} / F_{int} < 0.5$$

The two forces are calculated at the distance h corresponding to the force barrier.

By using a dimensionless form of (17), the characteristic time $\mu_c d^2 / \bar{F}$ appears ; then the association time and the coalescence efficiency may be written as :

$$t_{ass} \propto (\mu_c d^2 / \bar{F}) e^{F_{int}/\bar{F}} \quad (19)$$

$$\alpha^{coal} = \frac{k_{ass}}{k_{sep}} = \frac{t_{sep}}{t_{ass}} \propto \frac{\bar{F}}{\mu_c d^2 \dot{\gamma}} e^{-F_{int}/\bar{F}} \propto \frac{\bar{F}}{F_{sep}} e^{-F_{int}/\bar{F}} \quad (20)$$

3.1.2. Fragmentation

The fragmentation kernel can be written following Ross equation in [13] by :

$$K^{frag} = K_0^{frag} \alpha^{frag} \quad (21)$$

with

$$K_0^{frag} = \frac{P_i}{E_{turb}} \quad (22)$$

where P_i and E_{turb} are respectively the power input and the turbulence kinetic energy at the drop scale. P_i and E_{turb} are expressed by :

$$P_i = \rho_c \frac{\pi}{6} d^3 \varepsilon \quad (23)$$

$$\text{and } E_{turb} \propto \rho_c d^3 \overline{u^2} \propto \rho_c d^{11/3} \varepsilon^{2/3} \quad (d > \lambda_K) \quad (24)$$

Ross (in [13]), Tavlarides [13] and Luo [18] introduced into the fragmentation efficiency the ratio of the cohesion or the surface energy E_{coh} to the turbulence kinetic energy :

$$\alpha^{frag} = \exp\left(-\frac{E_{coh}}{E_{turb}}\right) \quad (25)$$

$$\text{with } E_{coh} \propto \sigma d^2 \quad (26)$$

Kostoglou et al. [19] used the Luo' formalism except that the cohesion energy was replaced by a threshold turbulence kinetic energy.

On the other hand, Sarimeseli [20] et al. proposed a rigorous modelling for drop fragmentation based on comparison between two characteristic times : the time t_{frag} needed for fragmentation and the contact time $t_{contact}$ between drop and eddies. The modelling leads to the following expressions :

$$K_0^{frag} \propto t_{contact}^{-1} \quad (27)$$

$$\text{and } \alpha_{frag} \propto \exp\left(-\frac{t_{frag}}{t_{contact}}\right) \quad (28)$$

$$\text{with } t_{contact} \propto d / \sqrt{u^2(d)} \quad (29)$$

$$\text{and } t_{frag} \propto \frac{\Delta p_{drop\ surface}}{\rho_c \varepsilon} \propto \frac{\sigma}{\rho_c \varepsilon d} \quad (30)$$

This modelling was close to Shamlou's approach [4], for whom the fragmentation efficiency might be written using the cohesion strength over fluid stress ratio :

$$\alpha_{frag} \propto \exp\left(-\frac{\Delta p_{drop\ surface}}{\Delta p_{contact}}\right) = \exp\left(-\frac{t_{frag}}{t_{contact}}\right) \quad (31)$$

$$\text{with } \Delta p_{contact} \propto \rho_c \varepsilon t_{contact} \propto \rho_c \varepsilon d / \sqrt{u^2(d)} \quad (32)$$

The same authors [18,20] proposed fragmentation kernels for drops in turbulent flow in the inertial sub-range. However, all the expressions contain the same dimensionless parameter : the Weber number of the drop We_d :

$$We_d = \frac{\rho_c \overline{u^2} d}{\sigma} = \frac{\rho_c \varepsilon^{2/3} d^{5/3}}{\sigma} \quad (33)$$

Several investigators defined a minimum diameter d_{min} and a maximum diameter d_{max} for an emulsion drop in a given turbulent medium : d_{min} corresponded to a very small value of efficiency α_{coal} and d_{max} to a very small value of efficiency α_{frag} . This is equivalent to the definition of d_{min} (d_{max}) by the equation $t_{coal} \square t_{contact}$ ($E_{coh} \square E_{turb}$ or $t_{frag} \square t_{contact}$).

So d_{max} obeys the relation $We_d(d_{max}) = We_{critical}$ for $d < \lambda_K$ or $d > \lambda_K$, which corresponds to the well-known empirical relation [13] for emulsion in a stirred tank :

$$d_{32} / D_a = 0.05 We^{-0.6} \quad (34)$$

$$\text{with } We = \frac{\rho_c N^2 D_a^3}{\sigma}$$

d_{32}, D_a, N are respectively the Sauter diameter of the drop, the impeller diameter and the stirrer speed.

The limit size for colliding rigid drops d_{min} obeys the relation :

$$d \propto \dot{\gamma}^{-1/2} \quad d < \lambda_K \quad (35)$$

As a summary, modelling of emulsion dynamics involves at once fragmentation kernel and zero collision efficiency to explain the limit drop size. The occurrence of a limit size without using fragmentation modelling is due to a coalescence efficiency including an exponential function. The characteristic time or force ratio seems the more appropriate one to represent coalescence or fragmentation.

3.2. Bubble-particle system

We consider a large bubble rising in a suspension of solid particle. This is equivalent to the motion of small particles towards the bubble. In the following d_p and d_b are respectively the particle diameter and the bubble diameter, u_b is the rising bubble velocity. The particles move along the streamlines, go around the bubble, slide on the surface of the bubble and are captured. So the whole process, called collection, is divided into three successive steps : collision or approach, attachment and bubble-particle set evolution, i.e stability. We might define a collection or aggregation kernel, but investigators preferred to introduce quantities such as probability or efficiency. The collection efficiency contains the efficiencies for each step :

$$E = E_c E_a E_s \quad (36)$$

E_c , E_a , E_s are respectively the efficiencies for collision, attachment and stability. The collision efficiency is proportional to the collision kernel $K_{0,i,j}^{agg}$. As collision efficiency is strongly depending on hydrodynamics of rising bubble, we will stop the analogy with particle suspension in other hydrodynamic conditions. At the contrary, attachment efficiency is exactly the aggregation efficiency $\alpha_{i,j}^{agg}$. The stability efficiency is another way to consider fragmentation in an aggregation process, as already done by Brakalov. Hence, we will focus our attention on attachment and stability efficiencies.

Dai [21] and Yoon [22] defined the contact time as the sliding time t_{sl} of the particle on the bubble surface and compared it to an induction time t_i , which is the time needed for rupture of the liquid film and the formation of the G-L-S contact line.

The induction time corresponds to the drainage of the liquid film due to macroscopic forces. When the film thickness reaches a critical value, (short range) interaction forces can lead to a very fast rupture of the film. Simple expression for t_i is available :

$$t_i \propto A(\psi)d_p^{0.6} \quad (37)$$

where ψ is the wetting angle of the G-L-S system.

As efficiency is related to cross section in this case, attachment efficiency obeys the relation :

$$E_a = \left(\frac{\sin \vartheta_a}{\sin \vartheta_t} \right)^2 \quad (38)$$

where ϑ_t is the maximal angle measured from the vertical axis for particle capture by bubble (i.e. $E_a = E_s = 1$) and ϑ_a with $\vartheta_a < \vartheta_t$ is the actual angle considering attachment phenomenon.

ϑ_a is such that the sliding time between ϑ_a and ϑ_t equals the induction time :

$$t_i = \int_{\vartheta_a}^{\vartheta_t} \frac{d_p + d_b}{2u_{\tan g}} d\vartheta \quad \text{and} \quad u_{\tan g} = \frac{2}{d_b} \frac{dZ}{\sin \vartheta dr} \quad (39)$$

$u_{\tan g}$ is the velocity along a streamline and Z is the stream function for the flow around the bubble. Hence, we may write Dai's theoretical result for the attachment efficiency as :

$$E_a = f \left(\left(d_p / d_b \right)^n t_{coal} / t_{contact} \right) \quad (40)$$

with $f(x) = \sin^2 \left(2 \operatorname{atan} \left(e^{-3\pi x/4} \right) \right)$; $t_{coal} = t_i$; $t_{contact} = \pi (d_p + d_b) / (4u_b)$

The exponent n is respectively equal to 0 for a large bubble ($d_b > 1\text{mm}$) and to 1 for a small bubble ($d_b < 0.1\text{mm}$).

In turbulent medium, Li [23] proposed an expression similar to Ross's for drop coalescence (Eq. 11):

$$E_a \approx e^{-\frac{t_i}{t_{contact}}} \quad \text{with} \quad t_{contact} \approx \frac{d_p + d_b}{\sqrt{u^2 (d_p + d_b)}} \quad (41)$$

Thus, as seen in (40) and (41), the attachment efficiency, i.e. aggregation efficiency, is a function of the ratio of coalescence and contact times.

It exists another approach considering short range interaction forces (attractive and repulsive). In most cases, the total interaction potential $V_T(h)$ presents a maximum $V_{T,\max}$ for a separation distance value denoted h_{\max} and a primary minimum denoted $-W_a$, W_a being the adhesion work. Song [24] suggested that the potential barrier was linked to the attachment efficiency, whereas the energy gap between primary minimum and maximum was related to the stability efficiency. Then, attachment efficiency was expressed as :

$$E_a = e^{-\frac{V_{T,\max}}{W_c}} \quad (42)$$

where W_c is the kinetic energy of the particle at $h = h_{\max}$; its value was coming from the analysis of the particle trajectory.

The stability efficiency was expressed as :

$$E_s = 1 - e^{-\frac{W_a + V_{T,\max}}{W_c'}} \quad (43)$$

where W_c' is the kinetic energy of the particle attached to the bubble. The adhesion work was written by means of macroscopic quantities :

$$W_a = \sigma \frac{\pi d_p^2}{4} (1 - \cos \psi)^2 \quad (44)$$

where σ is the surface tension for liquid-gas system.

However, Bloom [25] expressed the stability efficiency by means of a Bond number, which was defined as a ratio between repulsive force due to inertia in turbulent flow and attractive force due to capillarity :

$$Bo \square \frac{\rho_p \frac{\pi d_p^3}{6} a}{F_C} \quad (45)$$

acceleration a was written :

$$a \square \overline{u^2 (d_p + d_b)} / (d_p + d_b)$$

$$E_s = 1 - e^{1-Bo^{-1}} \quad (46)$$

Analysis of the different modelling shows a great disparity in the expressions (40-42) of the attachment efficiency. Equation (40), contrary to (41) and (42), takes into account the geometry of the system. Conversely (41) and (42) consider attachment as a stochastic process ; they are more convenient in turbulent medium. However (40) and (41) involve time whereas (42) involves energy. Stability efficiency uses either energy ratio (43) or force ratio (45).

4. Particle-particle system

Many investigators have studied aggregation of micronic particles under shear flow, i.e in a Couette flow or in a turbulent flow. Generally chemical conditions are such that only attractive forces act between particles, and that the size of formed aggregates is smaller than the Kolmogorov scale for turbulent aggregation. Aggregation occurs in the smallest eddies which are characterized by a shear rate expressed by :

$$\dot{\gamma} \propto (\varepsilon / \nu)^{1/2} .$$

4.1. Aggregation kernel

The kernel $K_{0,i,j}^{agg}$ is currently written as ([14],[26]) :

$$K_{0,i,j}^{agg} = \frac{4}{3} \dot{\gamma} (a_i + a_j)^3 \quad (47)$$

Experimental and theoretical results are known about :

- the aggregation efficiency for collisions between primary particles $\alpha_{1,1}^{agg}$ and between aggregates $\alpha_{i,j}^{agg}$,
- the fractal dimension of aggregates,
- the $a_L - \dot{\gamma}$ relation (expressed as $\frac{a_L}{a_1} \propto \dot{\gamma}^{-m}$),
- the characteristic time of aggregation expressed as $B(\dot{\gamma}\phi)^{-1}$ or $B(\alpha_{1,1}^{agg}\dot{\gamma}\phi)^{-1}$, where ϕ is the solid volume fraction in suspension and B a constant. This corresponds to the time needed for the aggregate to reach the limit size a_L .

For instance, aggregation efficiency for two equally sized micronic spheres is expressed as a function of the ratio of contact time and aggregation time :

$$C_A = \frac{A}{36\pi\mu\dot{\gamma}a^3} \quad (48)$$

where A is the Hamaker constant. This approach is similar to this one for coalescence of rigid drops. C_A can be seen as the ratio between attractive Van der Waals force and hydrodynamic resistance at surface-surface distance equal to particle radius.

But contrary to coalescence of drops, it has been theoretically shown [27] that the aggregation efficiency is better represented by a power law of C_A instead of an exponential law :

$$\alpha_{1,1}^{agg} \propto C_A^n \quad \text{with } 0 < n < 1 \quad (49)$$

The aggregation efficiency for two aggregates is more difficult to estimate. $\alpha_{i,j}^{agg}$ is a

function of $\frac{a_i}{\kappa_i^{1/2}}$, $\frac{a_j}{\kappa_j^{1/2}}$ and $C_A' = \frac{A}{36\pi\mu\dot{\gamma}a_{i,j,eq}^3}$. κ_i and $a_{i,j,eq}$ are respectively the

permeability of aggregates and an equivalent radius. For instance, the procedure proposed by Kusters *et al.* [2] (*shell-core* approach) has been successfully applied for aggregation of polystyrene latex, alumina, titania and silica suspensions. Kusters showed that aggregation between equally sized aggregates was favoured ([5], fig. 5.11) ; the corresponding aggregation efficiency can be approximated by :

$$\alpha_{i,i}^{agg} \approx 1.55 \left(\frac{a_i}{\kappa_i^{1/2}} \right)^{-0.43} \quad (50)$$

Gmachowski ([3], fig. 2) indicated that $\frac{a_i}{\kappa_i^{1/2}}$ was a single function of the fractal dimension which we will represent as :

$$\frac{a_i}{\kappa_i^{1/2}} \approx 6.6 (3 - D_f)^{-1.75} \quad (51)$$

Following the procedures of Kusters [2] and Vanni [28], the permeability can be evaluated.

According to these authors, $a_i / \kappa_i^{1/2}$ presents a weak dependence with the number of primary particles in aggregate :

$$\frac{a_i}{\kappa_i^{1/2}} \approx f(D_f) i^{0.19} \quad (52)$$

This expression will be preferred to the older one [6] :

$$\frac{a_i}{\kappa_i^{1/2}} \approx (0.6SD_f)^{1/2} (a_i / a_1)^{(D_f-1)/2}$$

then, (50) is reduced to

$$\alpha_{i,i}^{agg} \propto (a_i / a_1)^{-0.082D_f} \quad (53)$$

so for all researchers ([2],[3],[28]) $\alpha_{i,i}^{agg}$ is a very weak function of aggregate size.

Kusters [2] suggested that only the flows outside and inside the aggregates determined the aggregation efficiency. However, Van der Waals forces and hydrodynamic resistance could contribute to aggregation efficiency especially at the beginning of aggregation. So by analogy with (49) Kusters proposed to use :

$$\alpha_{i,i}^{agg} \propto C_A^m \quad (54)$$

as much as the value of $\alpha_{i,i}^{agg}$ was higher than the one given by (53).

Kusters [2] mentioned that the contribution of the two opposite primary particles, each one in each colliding aggregate, to Van der Waals forces was the most important . Hence, C_A' was expressed by ([2],[7],[29]):

$$C_A' = \frac{A}{36\pi\mu\dot{\gamma}a_i^3} \frac{a_1}{a_i} = C_A \frac{a_1}{a_i} \quad (55)$$

However we think that a more rigorous approach is possible. By considering Van der Waals interactions between all the primary particles of aggregates and the hydrodynamic radius of aggregates (see Appendix 1), we obtain :

$$C_A' = C_A 2^{1/D_f} (D_f/3)^5 (S^{1/D_f})^{2D_f-7} (a_1/a_i)^{6-2D_f+0.15/D_f} \quad (56)$$

Equations (55) and (56) have the same dependence for a_1/a_i if $D_f \square 2.53$. The proportionality constant is equal to 0.64. The value of fractal dimension proposed by Kusters ($D_f \square 2.5$) for turbulent aggregation is consistent with the above-written equations.

Hence, aggregation efficiency can be written as :

$$\alpha_{i,i}^{agg} \propto \dot{\gamma}^{-d} (a_i / a_1)^{-e} \quad (57)$$

$$\text{with } d = 0 \quad \text{and} \quad e = 0.082D_f \quad \text{for large aggregate} \quad (57a)$$

$$\text{with } d = n \quad \text{and} \quad e = n(9 - 2D_f + 0.15/D_f) \quad \text{for small aggregate} \quad (57b)$$

if $D_f = 2.5$ and $n = 0.18$, then e is equal to 0.2 for large aggregate or equal to 0.73 for small aggregate. This small value for exponent e is unable to explain the limit size reached by aggregates under shear.

By means of trajectory analysis Brakalov [7] calculated the collision efficiency from the following hypothesis :

- monosized, spherical and impenetrable aggregates
- interaction between the two opposite primary particles (as Kusters)
- existence of interparticle short-range repulsive forces.

The total force was expressed as :

$$F = F_{vw} (1 - (h_0 / h)^8) \quad (58)$$

F_{vw} was the Van der Waals force between two primary particles. h and h_0 were respectively the distance between the two particles and a fitting parameter. By using this force law, the limit size reached by aggregates corresponded to a vanishing collision efficiency without considering breakage.

4.2. Fragmentation kernel

Fragmentation kernel contains at once the fragmentation frequency and the fragmentation efficiency. Shear rate is often chosen as fragmentation frequency. However this is

amplified by a surface term if fragmentation mechanism is erosion. So fragmentation frequency can be written as :

$$K_{0,i}^{frag} = \dot{\gamma} (a_i / a_1)^r \quad (59)$$

with $0 < r < 1$ for breakage and $r = 2$ for erosion. The more evoked mechanism is breakage (Table 2).

Two kinds of expressions were proposed by investigators for fragmentation efficiency :

$$- \text{ exponential law : } \alpha_i^{frag} = e^{-R} \quad (60)$$

$$- \text{ power law : } \alpha_i^{frag} \propto R^{-q} \quad (q > 0) \quad (61)$$

$$\text{with } R = \sigma_s / \tau_s$$

τ_s and σ_s were respectively the shear stress and the cohesion strength. They obeyed the relations [4] :

$$\tau_s = \mu \dot{\gamma} \quad (62)$$

$$\sigma_s \propto 15 / (4\pi) \phi^{2.2} F_{adh} / a_1^2 \text{ with } \phi = S (a_i / a_1)^{Df-3} \quad (63)$$

F_{adh} was the adhesion force between primary particles in aggregate. Equation (60) is similar to (31) for drop fragmentation.

Equations (59) and (61) are consistent with the fragmentation kernel expressed as :

$$K_i^{frag} \propto \dot{\gamma}^b (a_i / a_1)^p \quad (64)$$

$$\text{with } b = 1 + q \text{ and } p = 2.2q(3 - Df) + r$$

Equation (64) is often used by researchers.

Table 1 gathers a few representative experimental results about characteristics of aggregation-fragmentation. Materials were either micronic polymer latex or metallic oxide particles. Experiments were carried out in a Couette cell where the flow was laminar or in a stirred tank where the flow was turbulent. Ranges of shear rate were similar except for aggregation in viscous liquid [30]. Reported values are n , Df , B and m . Expressions for fragmentation kernel are also reminded. Thus we can see that the average values of n , Df , B and m are respectively about 0.3, 2.4, 10 and 0.5. Unfortunately due to difficulties for measuring aggregate size by optical methods all experimental results were not accurate.

Table 2 gathers the corresponding theoretical results. Values for n are in the range [0.1-0.2] whereas B value equals 10. Main theoretical results concerned the limit size for aggregates and the fragmentation kernel. The limit size was obtained either from comparison between aggregate cohesion and fluid motion ([6], [46-48]) or from competition between aggregation and fragmentation dynamics ([5], [9], [50]). Two different criteria were used : one was based on energy, the other one on stress or force. Investigators did not bring out reasons or proofs about their choice. Another uncertainty concerns the use of fragmentation and its kernel in order to describe a whole aggregation process under shear flow. Modelling of Shamlou [4] and Subbanna [49] rested on equation (60). Conversely, modelling of Serra [33-35], Spicer [36] and Lu [50] used equation (61) with q respectively equal to 0.75, 0.6 and 1. The same authors used equation (64) with p respectively equal to 1, 1 and 4.

4.3. Aggregation dynamics and final size of aggregate

Aggregation dynamics can be modeled by three ways.

i.) The first one uses equations (2) and (7) for aggregation and fragmentation kernels. A steady state has been experimentally observed and theoretically [51] showed for long time.

The relation between the m-exponent and the two kernels can be obtained by the following arguments.

Assuming the inequality $\alpha_{i,j}^{agg} \square \alpha_{i,i}^{agg}$, let us choose a hierarchical model to describe aggregation :

$$2 A_1 \leftrightarrow A_2$$

$$2 A_2 \leftrightarrow A_4$$

$$2 A_j \leftrightarrow A_{2j} \quad j \leq L$$

A_j is an aggregate with j primary particles. The steady state is characterized by :

$$W_1 = W_2 = W_j \dots = 0$$

$$\text{with } W_j = -K_{j,j}^{agg} N_j^2 + K_{2j}^{frag} N_{2j}$$

The maximum of steady state PSD corresponds to aggregates with k primary particles :

$$N_{k/2} \square N_{2k} \text{ and } W_{k/2} = W_k = 0$$

thus,

$$N_k = \left(K_{2k}^{frag} / K_{k,k}^{agg} \right)^{2/3} \left(K_k^{frag} / K_{k/2,k/2}^{agg} \right)^{1/3}$$

$$\text{as } N_{1,0} = \sum_i i N_i \square k N_k$$

Hence by using equations (47), (57) and (64) :

$$k \propto K^{agg} / K^{frag} \propto \dot{\gamma}^{1-d} k^{(3-e)/Df} / \dot{\gamma}^b k^{p/Df}$$

$$\text{and } a_L \propto a_k \propto \dot{\gamma}^{(1-b-d)/(Df-3+e+p)} \quad (65a)$$

$$\text{then } m = (d+q) / ((Df-3)(1-2.2q) + e+r) \quad (65b)$$

The condition expressed as $k \propto K^{agg} / K^{frag}$ can be interpreted as the comparison of aggregation time T^{agg} to fragmentation time T^{frag} .

Kostoglou [51] used a similarity method in order to study the steady state for the case where $d = e = 0$. He deduced that :

- the steady state exists if $Df - 3 + p > 0$
- the standard deviation of the PSD, assumed as lognormal, is a function of Df , p , n_F (fragments number after fragmentation). The PSD is not depending on $\dot{\gamma}$ [36].
- $a_k \propto \dot{\gamma}^{(1-b)/(Df-3+p)}$ (66)

Equations (65a) and (66) are equivalent for $d = e = 0$. By comparing the calculations with the experiments Kostoglou et al. found out $p = 1.5$.

ii.) Alternately to the first modelling, the second modelling uses alternately a stability efficiency $E_{s,i+j}$ without fragmentation :

$$K_{i,j}^{agg} = K_{0,i,j}^{agg} \alpha_{i,j}^{agg} E_{s,i+j} \quad \text{and} \quad K_i^{frag} = 0 \quad (67)$$

$E_{s,i+j}$ can be a step function or a continuous decreasing function of $i+j$ -aggregate size. This approach was already used for bubble-particle systems (43,46) and for particle-particle systems to a certain extent by Brakalov [7].

So applying Bloom's approach (equation (46)) in the case of shear aggregation and using equations (62) and (63) for repulsive and attractive forces one may write :

$$F_{rep} / F_{att} \propto R^{-1}$$

The limit size a_L corresponds to :

$$R = 1 \quad (\text{or } E_{s,i+j} = 0)$$

Thus, from equations (8), (62) and (63) :

$$m = 1 / (2.2(3 - Df)) \quad \text{and} \quad E_{s,i+j} = 1 - e^{-1 - (a_{i+j}/a_L)^{-1/m}} \quad i + j \leq L \quad (68)$$

It should be noted that the stability efficiency as expressed in (46) and (68) is related to the fragmentation efficiency by :

$$\alpha_{i+j}^{frag} + E_{s,i+j} \leq 1 \quad (69)$$

This can also be seen in Table 2 ([4],[49]).

iii.) The third modelling (Kusters) uses stability efficiency $E_{s,i+j}$ in the aggregation kernel and the fragmentation kernel (equation (69)).

5. Discussion and conclusion

One may compare the different expressions for the m-exponent established by Sonntag [6], Mills [47-48], Bache [46] and the author ((65b) and (68)). According to all investigators, as the fractal dimension increases in the range [0;2.6], m increases in the range [0;1]. Expression of Mills and (68) contain only one parameter : the fractal dimension.

On the contrary, Sonntag's and Bache's expressions contain the exponents r_1 or r_2 which appear in ϕ -dependence of aggregate mechanical properties. r_1 and r_2 are close linked by the relation $r_2 = 2r_1 - 1$. Mills' equation corresponds to $r_2 = 2$. High (=5) or low (=1) value of r_1 corresponds respectively to a strong or a weak sensitivity of mechanical property with the solids volume fraction. As the solids volume fraction has the smallest value at the surface of aggregates, the strong sensitivity corresponds to an important weakness at the surface, i.e leads to an erosion or to small fragments loss from the surface. Fresh prepared

aggregates are characterized by intermediate values of r_1 ($2 < r_1 < 3$), whereas aged aggregates have higher values of r_1 ($r_1 > 4$). The former are formed during a fragmentation-aggregation process whereas the latter are made by restructuring of the former.

Equation (65b) contains several other parameters : n , r (characterizing erosion or breakage) and q . Their standard values can be taken as : $n = 0.3$; $r = 1$; $q = 1$ (q is in the range [0.6;1.2];see Table 1).

Figure 1 represents the curves of m -exponent versus the fractal dimension from Sonntag ($r_1 = 2.5$), Mills, equation (68), equation (65b) for small aggregates ($r = 1$) and equation (65b) for large aggregates ($r = 1$). Expressions of Sonntag and (65b) for small and large aggregates lead to similar results. In the case of shear aggregation ($D_f = 2.4$), m is found in the range [0.43-0.52]. Expression of Mills and equation (68) overestimate m . Higher value of r_1 ($r_1 > 4$) has the same effect, i.e. smaller value of m , than high value of r ($r = 2$).

Figure 2 represents the curves of m -exponent versus the fractal dimension from Sonntag ($r_1 = 4.5$), equation (65b) for small aggregates ($r = 2$) and equation (65b) for large aggregates ($r = 2$). For shear aggregation ($D_f = 2.4$), m is found in the range [0.3-0.34].

On the table 1, experimental values for m look like scattered. However two ranges of values appear : [0.25-0.35] and [0.5-0.75]. The first one can be associated to weak forces between primary particles, i.e due to small size or small Hamaker constant. In this case, erosion or small fragments loss from the surface predominate [6]. The second one corresponds to stronger interaction between primary particles and to larger aggregates.

Equation (65b) rests on aggregation-fragmentation dynamics, i.e the comparison of two times : collision-aggregation time and fragmentation time. Equation (68) rests on stability of a freshly formed aggregate, i.e the comparison of two stresses or forces. Thus there is no reason to get the same $\dot{\gamma}$ -dependence of limit size a_L . Equation (65b) is coming from an accurate analysis of aggregation kernel which does not appear when deriving (68). Forces involved in Equation (68) only appear in fragmentation kernel. It can be noted that Scurati et al. [53] gave a similar $a_L - \dot{\gamma}$ law with exponent $m = 1/(3 - Df)$ in the case of aggregates coming from the fragmentation of dry aggregates in viscous fluid.

The modelling of steady state for emulsion and particle suspension can be compared. Applying the hierarchical model to emulsion and considering efficiencies expressed as exponential function one obtains :

$$\frac{T^{frag}}{T^{coal}} = K^{coal} N / K^{frag} = 8C_V / \pi \exp\left(\frac{t_{frag} - t_{coal}}{t_{contact}}\right) \ll 1 \quad (70)$$

where C_V is the drop volume fraction in emulsion.

The characteristic time T^{coal} coming from the population balance equation is different from the time issued from individual collision t_{coal} . However, both (T^{coal}, T^{frag}) are related to

(t_{coal}, t_{frag}) by an unique way (Eq. 70). If efficiencies are very weak, then $\frac{T^{frag}}{T^{coal}} \ll \frac{t_{frag}}{t_{coal}} \ll 1$.

This approach would be correct only if coalescence and fragmentation could occur at the same time. However it seems that it is not the case for emulsion where depending on the initial state either coalescence or fragmentation would occur. Thus only the ratios $\frac{t_{coal}}{t_{cont}}$ or

$\frac{t_{frag}}{t_{cont}}$ determine the limit size. It can be emphasized that the ε -dependence of the drop limit

diameter in the inertial range of turbulence is not so different for the two cases : $d \propto \varepsilon^{-2/5}$ for fragmentation and $d \propto \varepsilon^{-5/17}$ for coalescence-fragmentation.

The different dynamics of emulsion and particle suspension are probably due to the higher sensitivity with the size of collision efficiency and fragmentation efficiency in the case of emulsion.

We described two ways in order to modelize the whole aggregation process, i.e. either by using an aggregation kernel (2) and a fragmentation kernel (7) or by introducing a stability efficiency (67) into the aggregation kernel (2). The two modelling contain the same ingredients. However the $a_L - \dot{\gamma}$ dependences are different. The analysis of the behaviour of other dispersed media and the agreement of the modelling of particles aggregation with experiments show that the best representation involves fragmentation.

APPENDIX

Following the procedure of Hamaker for the calculation of Van der Waals interaction potential U_{12} between two equally sized porous macroscopic bodies (denoted 1 and 2), one derive :

$$U_{12} = \int_u^1 \int_u^1 4A\phi_a(r_1)\phi_a(r_2) f(r_1, r_2, h) r_1^2 r_2 / h dr_1 dr_2 \quad (\text{A1})$$

with

$$u = a_1 / a_i$$

$$f = f_1 + f_2 + f_3 + f_4$$

$$f_1 = 1/2 \left(r_1^2 - (r_2 - h)^2 \right)^{-2}$$

$$f_2 = -1/2 \left(r_1^2 - (r_2 + h)^2 \right)^{-2}$$

$$f_3 = -2/3 r_1^2 \left(r_1^2 - (r_2 - h)^2 \right)^{-3}$$

$$f_4 = 2/3 r_1^2 \left(r_1^2 - (r_2 + h)^2 \right)^{-3}$$

All distances are made dimensionless by dividing them by the aggregate radius. h is the surface-surface distance. r_1 or r_2 are the distances between a given point of aggregate 1 or 2 and its centre. $\phi_a(r)$ is the volume density inside each aggregate. One deduce an approximated expression for Van der Waals forces between two aggregates separated by $h = 1$, which is suitable for comparison with other results :

$$F_{vw}(a_i, a_1, D_f) \square F_{vw}(a_i) (D_f / 3)^5 (S^{1/D_f})^{2D_f - 6} (a_i / a_1)^{2D_f - 6} \quad 1.6 < D_f < 3 \quad (\text{A2})$$

$F_{vw}(a_i)$ corresponds to the Van der Waals force between non porous spheres with the same outer diameter a_i .

The hydrodynamic resistance for fractal aggregates has been studied by Vanni [28] and Gmachowski [3]. It is expressed by using a corrective drag coefficient Ω_i , which is a function of D_f and a_i/a_1 . By using Neale and Veerapaneni's work, Vanni [28] shows that a good approximation for Ω_i ($D_f > 2$) is :

$$\Omega_i = \frac{2\beta^2(1 - \frac{\tanh \beta}{\beta})}{2\beta^2 + 3(1 - \frac{\tanh \beta}{\beta})} \text{ with } \beta = \frac{a_i}{\kappa_i^{1/2}} \quad (\text{A3})$$

where κ_i is the aggregate permeability at the aggregate surface.

It is not possible to find such a simple expression for Ω_i for $D_f < 2$; Some authors assume that Ω_i only depends on the fractal dimension. Thus, Gmachowski, [3], from different considerations, suggests the following expression :

$$\Omega_i = S^{1/D_f} \quad (\text{A4})$$

The difference between the two approaches is a weak dependence on a_i/a_1 for the expression of Vanni. From the Vanni's work (figure 7), one can approximate the corrective drag coefficient by the simple expression :

$$\Omega_i \approx S^{1/D_f} 2^{-1/D_f} (a_i/a_1)^{0.15/D_f} \quad 10 < a_i/a_1 < 10^3 \quad (\text{A5})$$

Hence,

$$C'_A = \frac{F_{vw}(a_i, a_1, D_f)}{6\pi\mu a_i (\dot{\gamma} a_i) \Omega_i} = C_A \frac{F_{vw}(a_i, a_1, D_f)}{F_{vw}(a_i) \Omega_i} = C_A 2^{1/D_f} (D_f/3)^5 (S^{1/D_f})^{2D_f-7} (a_1/a_i)^{6-2D_f+0.15/D_f} \quad (\text{A6})$$

REFERENCES

1. Kyriakidis, A.S., Yiantsios, S.G., and Karabelas, A.J., *J. Coll. Interface. Sci.*, **195**, 299 (1997).
2. Kusters, K. A., Wijers, J. G., and Thoenes, D., *Chem. Eng. Sci.*, **52**, 107 (1997).
3. Gmachowski, L., *J. Coll. Interface Sci.*, **178**, 80 (1996)
4. Ayazi Shamlou, P., Stavrinides, S., Titchener-Hooker, N. and Hoare, M., *Chem. Eng. Sci.*, **49**, 2647 (1994).
5. Kusters, K. A., "The influence of turbulence on aggregation of small particles in agitated vessel ", Ph.D. Thesis, Eindhoven University of Technology, The Netherlands (1991).
6. Sonntag, R. C., and Russel, W. B., *J. Coll. Interface Sci.*, **115**, 378 (1987).
7. Brakalov, L.B., *Chem. Eng. Sci.*, **42**, 2373 (1987).
8. Selomulya C., Bushell G., Amal R. and Waite T.D., *J. Coll. Interface Sci.*, **236**, 67(2001).
9. Selomulya C., Bushell G., Amal R. and Waite T.D., *Chem. Eng. Sci.*, **58**, 327(2003).
10. Gmachowski L., *Colloids & Surfaces A : Physicochemical and Engineering Aspects*, **207**, 271(2002).
11. Chakraborti R.K., Gardner K.H., Atkinson J.F., Van Benschoten J.E., *Water Res.* **37**, 873(2003).
12. Gruy, F., *J. Coll. Interface Sci.*, **237**, 28 (2001)
13. Tavlarides L.L., Stamatoudis M., *Advances in Chem. Eng.* **11**, 199(1981).
14. Saffman, P. G., and Turner, J. S., *J. Fluid Mech.*, **1**, 16 (1956).

15. Abrahamson, J., *Chem. Eng. Sci.*, **30**, 1371(1975)
16. Narsimhan G., *J. Coll. Interface Sci.*, **272**, 197(2004).
17. Zeichner, G. R., and Schowalter , W. R., *AIChE J.*, **23**, 243 (1977).
18. Luo H., Svendsen H.F., *AIChE J.*, **42**, 1225(1996).
19. Kostoglou, M. and Karabelas, A.J., *Chem. Eng. Sci.*, **60**, 6584(2005)
20. Sarimeseli A., Kelbaliyev G., *Chem. Eng. Sci.*, **59**, 1233(2004).
21. Dai Z., Fornasiero D., Ralston J., *J. Coll. Interface Sci.*, **217**, 70(1999).
22. Yoon R.H., Luttrell G.H., *Min. Proc. & Extr. Metall. Rev.*, **5**, 101(1989).
23. Li D., Fitzpatrick J.A., Slattery J.C., *Ind. Eng. Chem. Res.*, **29**, 955(1990).
24. Song S., Lopez-Valdivieso A., *J. Coll. Interface Sci.*, **212**, 42(1999).
25. Bloom F., Heindel T.J., *Math. Comput. Modelling*, **25**, 13(1997).
26. De Boer, G. B. J., Hoedemakers, G. F. M. and Thoenes, D., *Chem. Eng. Sci.*, **67**, 301 (1989).
27. Van de Ven, T. G. and Mason, S. G., *Colloid and Polymer. Sci.*, **255**, 468 (1977).
28. Vanni M., *Chem. Eng. Sci.*, **55**, 685(2000).
29. Sato, D., Kobayashi, M., and Adachi, Y., *J. Coll. Interface. Sci*, **272**, 345 (2004).
30. Chimmili, S., Doraiswamy, D., and Gupta, R.K., *Ind. Eng. Chem. Res.* **37**, 2073 (1998).
31. Nakaoka, T., Tanigushi, S., Matsumoto, K., Johansen, S.T., *I.S.I.J. International*, **41**, 1103(2001).
32. Oles, V., *J. Coll. Interface Sci.*, **154**, 351 (1992).
33. Serra, T. and Casamitjana, X., *AIChE J.*, **44**, 1724 (1998).

34. Serra, T. and Casamitjana, X., *J. Coll. Interface Sci*, **206**, 505 (1998).
35. Serra, T., Colomer, J., and Casamitjana, X., *J. Coll. Interface Sci*, **187**, 466 (1997).
36. Spicer, P.T., Pratsinis, S.E., Raper, J., Amal, R., Bushell, G., Meesters, G., *Powder Tech.* **97**, 26(1998).
37. Chin, C.J., Yiacoumi, S., Tsouris, C., *J. Coll. Interface Sci*, **206**, 532 (1998).
38. Tontrup T., “ Granulométrie de particules fines en suspension chargée par mesures de rétrodiffusion de lumière ” Ph.D. Thesis, Ecole des Mines de Saint-Etienne, France (1999).
39. Peng, S.J., and Williams R.A., *J. Coll. Interf. Sci.*, **166**, 321 (1994).
40. Gruy, F. and Cournil M., *Part. Part. Syst. Charact.*, **20**,1 (2004)
41. Brunk, B.K., Koch, D.L., and Lion, L.W., *J. Fluid Mech.*, **364**, 81 (1998).
42. Potanin, A.A., *J. Coll. Interface Sci*, **145**, 140 (1991).
43. Hounslow, M., *International Symposium Industrial Crystallization*, Sorrento, 2002.
44. Spicer, P. T., and Pratsinis, S. E., *AIChE J.*, **42**, 1612 (1996).
45. Higashitani. K., Iimura. K., *J. Coll. Interface Sci.* **204**, 320(1998).
46. Bache, D.H., *Chem. Eng. Sci.*, **59**, 2521(2004).
47. Mills, P., *J. Phys. Lett.*, **46L**, 301(1985).
48. Adler, P.M., Mills, P., *J. of Rheology* **23**, 25(1979).
49. M. Subbanna M., Pradip, S.G. Malghan, *Chem. Eng. Sci.*, **53**, 3073(1998).
50. Lu, S., Ding, Y., Guo, J., *Advances in Colloid and Interf. Sci.*, **78**, 197(1998).

51. Kostoglou, M., Karabalas, A.J., *J. Aerosol. Sci.*, **30**, 157(1999).
52. Bohin, F., Manas-Zloczower, I. and Feke, D.L., *Chem. Eng. Sci.*, **51**, 5193(1996)
53. Scurati, A., Feke, D.L. and Manas-Zloczower, I., *Chem. Eng. Sci.*, **60**, 6564(2005)

TABLES

Table 1 : experimental results for aggregation-fragmentation

L : laminar (Couette flow) T : turbulent (stirred tank)

PS : polystyrene latex

Table 2 : theoretical results for aggregation-fragmentation

LA : laminar aggregation TA : turbulent aggregation

LF : laminar fragmentation TF : turbulent fragmentation

β : percentage of broken links between primary particles in aggregate

E : binding energy between primary particles

σ : attractive force between primary particles per area unit in aggregate

r1 : exponent in ϕ -dependence of elastic shear

r2 : exponent in ϕ -dependence of volumic cohesive energy

* X_{agg} is differently defined in the Bache's paper.

FIGURES

Figure 1 : m -exponent versus fractal dimension from different modelling
Case 1 : small values for r_l and r .

Figure 2 : m -exponent versus fractal dimension from different modelling
Case 2 : high values for r_l and r .

Authors	n	D_f	B	$m,$ $\frac{a_L}{a_1} \propto \dot{\gamma}^{-m}$	K^{frag}	Experimental system
Chimmili [30]	0.7			0.56		L/Glass beads ; 4 μ m viscous medium $3 < \dot{\gamma}(s^{-1}) < 30$
Sonntag [6]		2.48		0.35		L; PS ; 0.14 μ m $1800 < \dot{\gamma}(s^{-1}) < 6000$
Selomulya [8,9]		[2.45-3]	1.2	0.28		T/PS ; 0.38 μ m $32 < \dot{\gamma}(s^{-1}) < 246$
Gruy [12,40]	0.4	2.4		0.25		T/SiO ₂ ; 0.5 μ m and 1.5 μ m $45 < \dot{\gamma}(s^{-1}) < 360$ small aggregates
Nakaoka [31]	0.24		6			T/PVT ; 2 μ m $40 < \dot{\gamma}(s^{-1}) < 200$
Oles [32]		[2.1-2.5]	8	\square 0.5		L/PS ; 2.2 μ m $25 < \dot{\gamma}(s^{-1}) < 150$
Serra [33-35]		2.24	7	0.7	$\propto \dot{\gamma}^{1.75} a_i / a_1$	L/PS ; 2 μ m or 5 μ m $25 < \dot{\gamma}(s^{-1}) < 195$
Brakalov [7]				0.55-0.6		Mg(OH) ₂ ; 0.022 μ m Fe(OH) ₂ ; 0.042 μ m $80 < \dot{\gamma}(s^{-1}) < 1200$
Spicer [36]	0	[2.3-2.65]	1	0.5-0.6	$\propto \dot{\gamma}^{1.6} a_i / a_1$	T/PS ; 0.87 μ m $60 < \dot{\gamma}(s^{-1}) < 130$ Large aggregates

Chin [37]	0.25 -0.3					T/PS ; 0.5 μ m-1 μ m $220 < \dot{\gamma}(s^{-1}) < 620$ small aggregates
De Boer [26]	0.36		20	0.5		T/PS ; 0.88 μ m $8 < \dot{\gamma}(s^{-1}) < 280$
Kusters [2]		2.5	13	0.75		T/PS ; 0.8 μ m $60 < \dot{\gamma}(s^{-1}) < 460$
Tontrup [38]		2.4		0.6		T/TiO ₂ ; 0.35 μ m $60 < \dot{\gamma}(s^{-1}) < 360$
Bohin [52]				0.5		L/SiO ₂ ; 2mm $25 < \dot{\gamma}(s^{-1}) < 170$ dry and homogeneous aggregate
Peng [39]				$a_L \propto \lambda_K$ $\propto \dot{\gamma}^{-1/2}$	$\propto \dot{\gamma}^2 d_i^{4-6}$	T/SiO ₂ ; 40 μ m Concentrated suspension $100 < \dot{\gamma}(s^{-1}) < 500$

TABLE 1 : experimental results for aggregation-fragmentation

L : laminar (Couette flow) T : turbulent (stirred tank)

PS : polystyrene latex

Authors	n	D_f	B	$\frac{a_L}{a_1} \propto \left(\frac{X_{agg}}{X_{fluid}} \right)^c \propto \dot{\gamma}^{-m}$	$K^{frag} \propto \dot{\gamma} \exp\left(-\frac{X_{agg}}{X_{fluid}}\right)$	Conditions <i>Criterion</i>
Brunk [41]	0.16					TA
Van de Ven [27]	0.18					LA
Potatin [42]	0.11					LA
Hounslow [43]	1					TA+growth <i>stress</i>
Spicer [44]			10			LA
Brakalov [7]				$m=[0.55-0.6]$		TA LA
Sonntag [6]				$m = 1 / (D_f - 1) / 2 + r_1 (3 - D_f)$ $\frac{a_L}{\kappa_L^{1/2}} < 10$ $m = 1 / r_1 (3 - D_f)$ $\frac{a_L}{\kappa_L^{1/2}} > 10$		LF Large aggregates <i>stress</i>
Higashitani [45]				[0.4-0.5]		LF $i < 100$ <i>stress</i>
Bache [46] *				$m = 2 / (2 + r_2 (3 - D_f))$ $c = 1 / (2 + r_2 (3 - D_f))$ $X_{fluid} \propto \rho a_1^2 \dot{\gamma}^2$ $X_{agg} \propto \beta E / (4 / 3 \pi a_1^3)$		Weak TF Large aggregates $D_f < 1.8$ <i>energy</i> $0 < d / \lambda_k < 3.5$
Mills [47,48]				$m = 1 / (4 - D_f)$ $c = 1 / (4 - D_f)$ $X_{fluid} = \mu \dot{\gamma}$ $X_{agg} \propto E / (4 / 3 \pi a_1^3)$		LA <i>stress</i>

Shamlou [4] Subbanna [49]					$X_{fluid} = \mu \dot{\gamma}$ $X_{agg} \propto \phi^{2.2} \sigma$	TF <i>stress</i>
Scurati [53]				$m = 1 / (3 - D_f)$		LF Large and dry aggregate <i>stress</i>
Kusters [5]		2.5			$X_{fluid} = (\mu \dot{\gamma})^2$ $X_{agg} \propto (\phi^{2.2} \sigma)^2$	TA <i>energy</i>
Selomulya [9]					$X_{fluid} = \varepsilon$ $X_{agg} \propto \dot{\gamma}^{1.7} (a_1 / a_i)$	TA, LA, TF, LF <i>energy</i>
Lu [50]				$a_i < \lambda_K$ $X_{fluid} = \mu \dot{\gamma}$ $X_{agg} \propto (a_1 / a_i)^2 \sigma$ $a_i \gg \lambda_K$ $X_{fluid} \propto (\varepsilon a_i)^{2/3}$ $X_{agg} \propto (\lambda_K / a_i) \sigma$	$K^{frag} \propto$ $\dot{\gamma} \left(\frac{X_{agg}}{X_{fluid}} \right)^{-1} a_i^2$ (erosion)	<i>stress</i>

TABLE 2 : theoretical results for aggregation-fragmentation

LA : laminar aggregation

TA : turbulent aggregation

LF : laminar fragmentation

TF : turbulent fragmentation

β : percentage of broken links between primary particles in aggregate

E : binding energy between primary particles

σ : attractive force between primary particles per area unit in aggregate

r1 : exponent in ϕ -dependence of elastic shear

r2 : exponent in ϕ -dependence of volumic cohesive energy

*** X_{agg} is differently defined in the Bache's paper.**

Figure 1

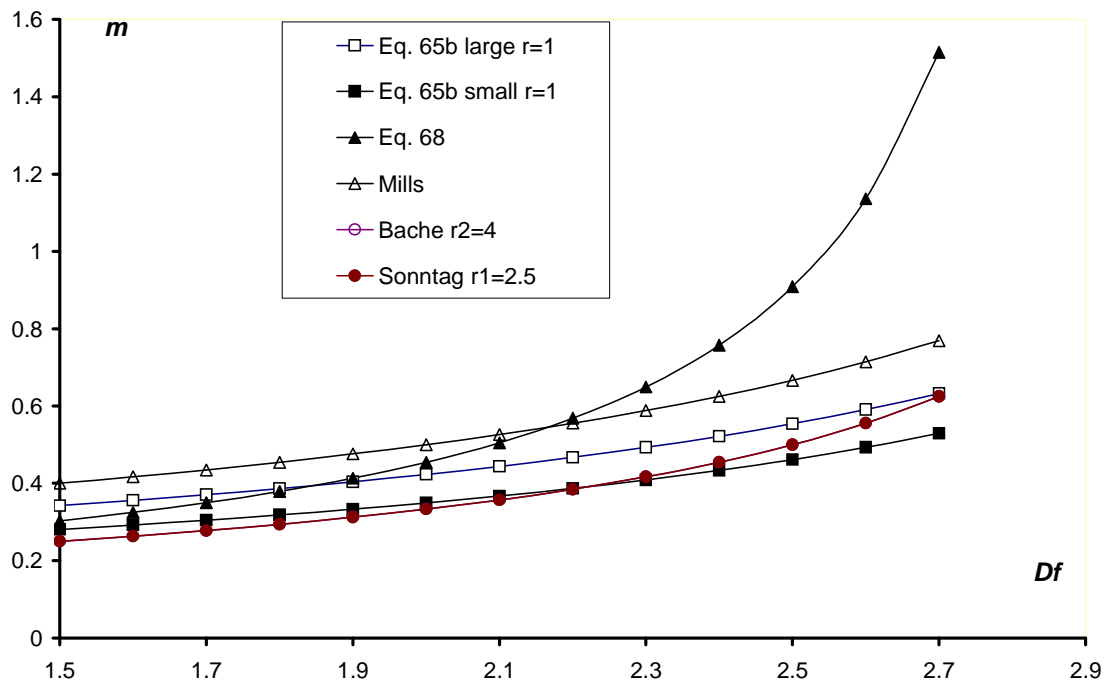


Figure 2

